

# Multi-rating Electronic Ballast for Fluorescent Lamps based on Operating Frequency Determination

Piyasawat Navaratana Na Ayudhya\* Non-member  
 Sumate Naetiladdanon\*\* Non-member  
 Anawach Sangswang\*\*\* Non-member

This paper presents an electronic ballast system with lamp rating detection capability. From the experimentally obtained operating frequency of the lamps, a possibility weight is constructed to help facilitate the lamp classification. The proposed detection algorithm employs a multi-step lamp power regulation algorithm where decision making is based on the sensed frequency and the possibility weight. Simulation and experimental results show that the proposed detection method can successfully detect the targeted lamp power rating and deliver the desired power to the lamp.

**Keywords:** ballast, fluorescent lamps, automatic detection, frequency determination

## 1. Introduction

Fluorescent lamps are commonly used in lighting applications because they consume less power than alternative lamps. Unlike incandescent lamps, fluorescent lamps always require a ballast to stabilize the lamp at the required operating point by limiting the discharge current<sup>(1)(2)</sup>. Simple magnetic ballasts that operate at the line frequency have many drawbacks, such as low efficiency, low input power factor and bulky size. However, electronic ballasts that employ transistors to boost line-frequency to high-frequency improve the lamp efficacy and system efficiency<sup>(3)</sup>. If the lamp is operated at a frequency higher than 20 kHz, instead of a line frequency of 50-60 Hz, the result is an increased light output (lumens) of 10-20%. The electronic ballast is often implemented as a series-parallel-loaded resonant inverter. This implementation can both ignite the lamp and supply the lamp as a current source at constant frequency<sup>(4)~(6)</sup>. The use of a power factor correction (PFC) AC-DC stage, specifically a boost rectifier operating in discontinuous conduction mode (DCM) with constant frequency and constant duty cycle, can achieve an input power factor close to unity. Moreover, modern electronic ballasts are implemented with microprocessor circuits, allowing control strategy implementation for energy savings and lamp protection features<sup>(7)</sup>.

Commercially available lamps, such as 18W, 32W and 36W T8 lamps, must be used with electronic ballasts specifically designed for each lamp power rating. A mismatch between ballast and lamp ratings usually results in damage to both the lamp and the ballast circuit,

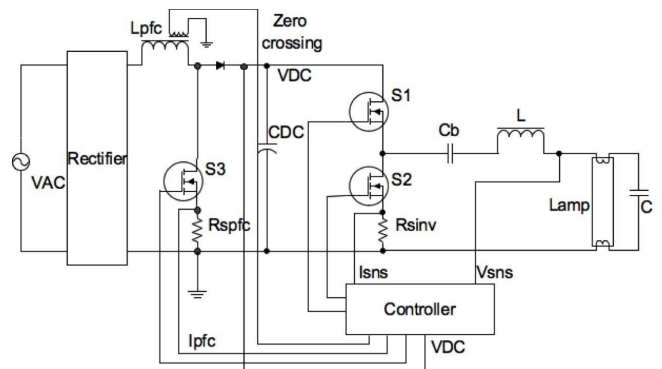


Fig. 1. Schematic of electronic ballast using in this paper

caused by over-current or hard switching<sup>(8)(9)</sup>. With a large number of different ratings of fluorescent lamps, an equally large stock of specifically rated electronic ballasts is required. The multi-rating fluorescent ballast is a solution to eliminate this problem. The controller of the multi-rating ballast must regulate and deliver the correct power to a lamp of unknown rating. Thus, the lamp rating detection algorithm must be accurate and sufficiently fast. The voltage detection method can differentiate between lamp power ratings by using the operating lamp voltage<sup>(10)(11)</sup>. However, the lamp voltage after striking (ignition) varies with the lamp temperature, age, and manufacturer. Thus, different lamp ratings may have overlapping voltage ranges. For example, 32WT8 and 58WT8 lamps operate at the same voltage, ranging from 117 V to 127 V, which can result in misidentification of the lamp. In addition, noise can interfere with the voltage, and adding a filter may increase the cost of the system.

This paper presents a multi-rating electronic ballast for fluorescent lamps based on operating frequency de-

\* King Mongkut's University of Technology Thonburi (KMUTT), Thailand, piyasawat.nav@kmutt.ac.th

\*\* KMUTT, sumate.nae@kmutt.ac.th

\*\*\* KMUTT, Anawach.San@kmutt.ac.th

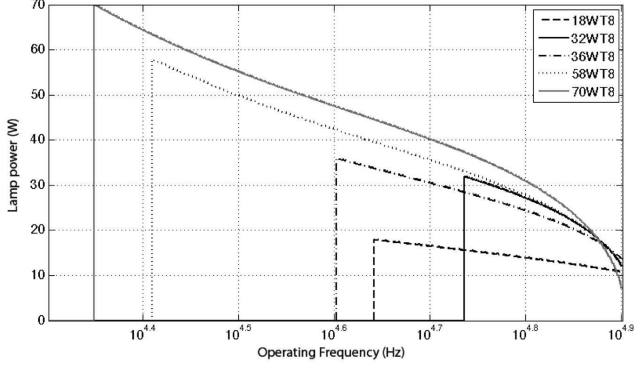


Fig. 2. Operating frequency VS Lamp power

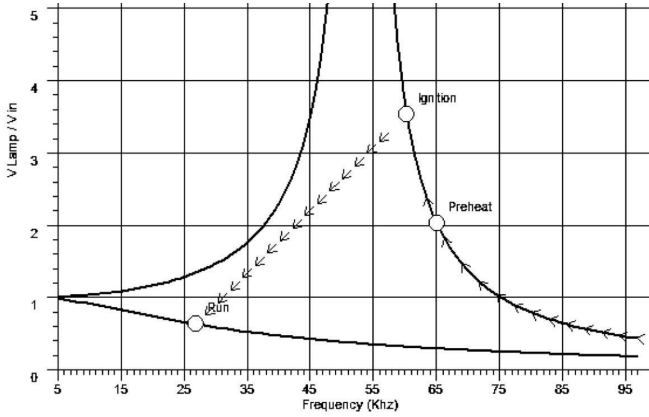


Fig. 3. Operating frequency vs. voltage gain (before and after striking)

termination. The paper includes the configuration and the controller design of a multi-rating electronic ballast. We propose a lamp rating detection algorithm, composed of multi-step lamp power regulation and the trapezoidal possibility weight determination<sup>(12)</sup> based on a given set of lamp operating frequency data. Finally, we present numerical and experimental results. A hardware prototype of the electronic ballast is carried out on an 8 bits micro-controller.

## 2. Multi-rating Electronic Ballast Configuration

The two-stage electronic ballast consists of a PFC boost rectifier and a half-bridge resonant inverter as shown in Fig. 1. By varying the inverter frequency, the ballast operates in pre-heat, strike, and running stages. The lamp current can be controlled through frequency variation as shown in Fig. 2<sup>(13) (14)</sup>.

Before ignition, the fluorescent lamp resistance is assumed to be infinite. By operating with frequency higher than the circuit resonant frequency, the current flows through the lamp filaments via the series capacitor. In this stage, the filaments are heated while the lamp voltage is not high enough to be ignited. After one second of preheating, the frequency is decreased to increase the output voltage gain until the lamp voltage is high enough to strike the lamp. Note that the relationship between the ballasts voltage gain and fre-

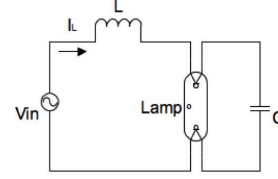


Fig. 4. Simplified resonant inverter for electronic ballast

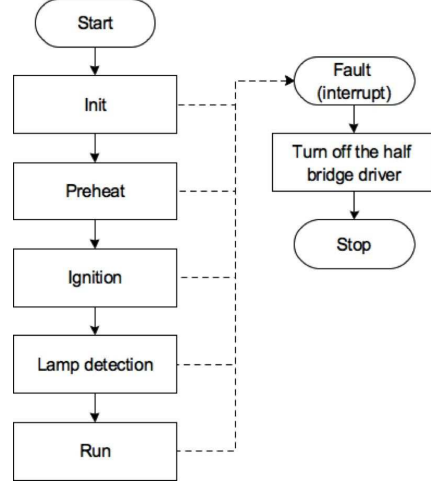


Fig. 5. Flowchart of the multi-rating electronic ballast operation

quency is shown in Fig. 3, obtained from the equivalent resistance of the lamp at steady-state condition using IR ballast designer software<sup>(15)</sup>.

Initially, the resonant circuit is in the high quality factor mode (High-Q). Once the lamp has been ignited, the lamp resistance decreases and exhibits a negative differential resistance behavior. This results in lamp voltage reduction and changes the resonant circuit condition to the low quality factor condition (Low-Q). At this stage, the lamp rating must be detected accurately. After this stage, the controller will command the switch signals to operate the ballast at proper frequency for the lamp.

**2.1 Half-bridge resonant inverter** By assuming that the resonant capacitor ( $C$ ) is only used for lamp preheating and striking while the resonant inductor ( $L$ ) is for limiting the lamp current, the values of  $L$  and  $C$  must be chosen to ensure the optimal power transfer of the low-Q RCL circuit. The resonant inverter input power ( $P_{inv}$ ) is<sup>(16) (17)</sup>,

$$P_{in} = V_{in} I_L = \frac{P_{lamp}}{\eta} \quad (1)$$

By using the simplified version of resonant inverter that shown in Fig. 4. The input voltage ( $V_{in}$ ) is the fundamental component of the square wave produced by the inverter<sup>(24)</sup>. This square wave is toggle between 0V and  $V_{DC}$ .

$$V_{in} = \frac{\sqrt{2}V_{DC}}{\pi} \quad (2)$$

$$\frac{P_{lamp}}{\eta} = V_{in} I_L = \frac{\sqrt{2}V_{DC}}{\pi} I_L \quad (3)$$

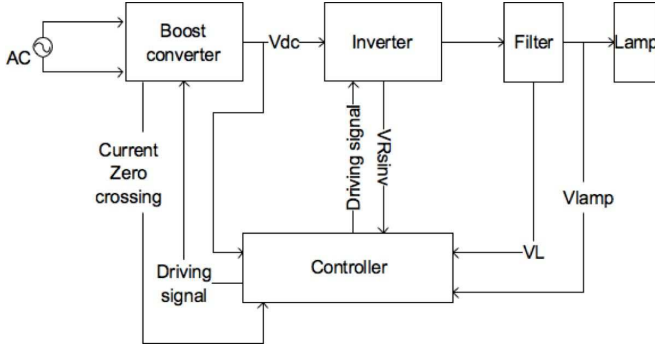


Fig. 6. Controller block diagram

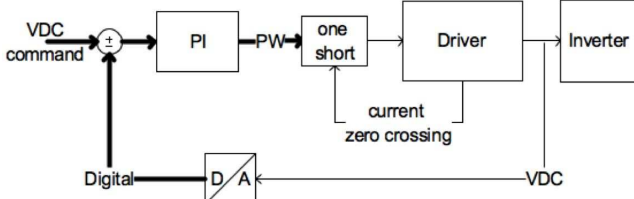


Fig. 7. DC bus voltage control

Where  $P_{lamp}$  is the power dissipated at the lamp;  $V_{DC}$  is the DC bus voltage, and  $\eta$  is the inverter efficiency. It is assumed that the inductor and lamp voltages are the same. The inductor current can be calculated by using a half of the DC bus voltage which results in,

$$I_L = \frac{V_{DC}}{4\omega L} \quad (4)$$

Thus:

$$P_{in} = \frac{\sqrt{2}V_{DC}}{\pi} \frac{V_{DC}}{4\omega L} = \frac{V_{DC}^2}{4\sqrt{2}\pi^2 f_{run} L} \quad (5)$$

From (3) and (5), the resonant inductance is:

$$L = \frac{V_{DC}^2 \eta}{4f_{run} \sqrt{2}\pi^2 P_{lamp}} \quad (6)$$

where  $f_{run}$  is the running or operating frequency. The controller is divided into two parts: the boost rectifier (DC bus voltage control), and the resonant inverter (lamp power control). These are shown in Fig. 7 and 8, respectively.

During preheat, the resistance of the lamp is infinite and the filament resistance is negligible. This results in an LC series circuit. Using the impedance across the capacitor, the peak preheat voltage  $V_{ph}$  is given as:

$$V_{ph} = \frac{I_{ph}}{2\pi f C} \quad (7)$$

where  $I_{ph}$  is the preheat lamp current and  $f$  is the preheat frequency. The transfer function is

$$V_{ph} = \frac{2V_{in}}{\pi (1 - 4\pi^2 f^2 LC)} \quad (8)$$

To preheat the lamp filament with the desired current while the lamp voltage is kept below  $V_{ph}$ , the resonant capacitance can be calculated from (8) as,

$$C = \frac{I_{ph}^2 L}{(V_{ph} + V_{DC}/\pi)^2 - (V_{DC}/\pi)^2} \quad (9)$$

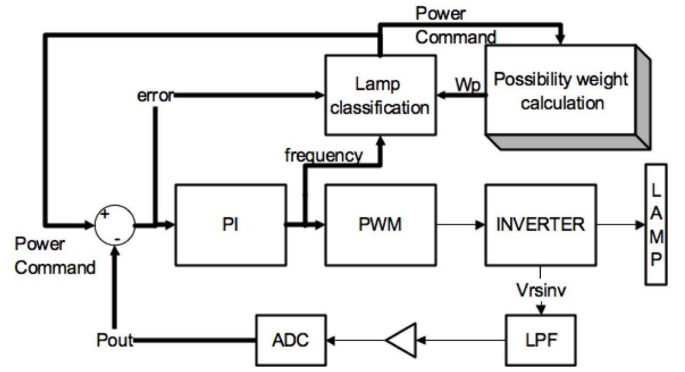


Fig. 8. Lamp power control with rating detection

**2.2 PFC boost rectifier** The PFC boost converter parameters are obtained by assuming an operation in the critical-conduction mode. With this control method, the PFC boost inductance is obtained from<sup>(17) (18)</sup>

$$L_{PFC} = \frac{8 \times 10^{-6} \eta V_{AC(rms)} (V_{DC} - \sqrt{2} V_{AC(rms)})}{2\sqrt{2} P_{OUT}} \quad (10)$$

where  $\eta$  is the target efficiency of the converter;  $V_{AC(rms)}$  is the minimum input RMS voltage and  $P_{OUT}$  is output power.

**2.3 Preheating condition** Although the multi-rating ballast has an advantage on that it can operate more than one lamp power ratings, the preheat condition is taken into account. According to<sup>(21)</sup>, the filaments must be operated at temperatures between  $700^\circ C$  and  $1000^\circ C$ , to avoid a premature wear of the emissive coating which will reduce the average life of the lamp. Since it is difficult to measure this temperature, there are recommendations and standards regarding correlated parameters, such as the voltage across the filaments and their equivalent resistances. Under appropriate temperature, the resistance of the filament should be in the range of 4.25 to 6.25 times of its resistance at room temperature<sup>(21) (22)</sup>. To increase the filament temperature, an electrical current is applied to the filament with the following relationship<sup>(19)</sup>.

$$R_{hc} (i_{ph(rms)}, t) = 1 + r_1 \left( e^{\left( \frac{i_{ph(rms)}}{r_2} \right)} - 1 \right) t \quad (11)$$

Where  $R_{hc}$  is the resistance ratio between hot resistance ( $R_c$ ) and cold resistance ( $R_h$ )

$i_{ph(rms)}$  is the filament current (A) during preheating

$t$  is the preheating time (s)

$r_1$  and  $r_2$  are the constants of the lamp

Note that for T8 series  $r_1$  and  $r_2$  are given as  $0.112 s^{-1}$  and  $0.155 A$ , respectively. In addition, the suitable preheating time should be in the range of 0.5 and 1.5 s. The minimum current is obtained as 467 mA using the  $R_{hc}$  value of 4.25 and the preheating time of 1.5 s from (11). Similarly, with the  $R_{hc}$  value of 6.25 and the preheating time of 0.5 s, the maximum current is given as 705.5 mA. As long as the  $i_{ph(rms)}$  is in between the men-

Table 1. Average running frequency of ballast at various lamp power ratings

Average of operating frequency at power command	16W (kHz)	30W (kHz)	34W (kHz)	56W (kHz)	68W (kHz)
T8-18	49.54	-	-	-	-
T8-32	76.26	55.44	-	-	-
T8-36	75.88	48.25	40.59	-	-
T8-58	76.26	57.16	50.09	25.21	-
T8-70	75.79	62.49	56.82	28.73	21.75

Table 2. Standard deviation of running frequency of ballast at various lamp power ratings

S.D. of operating frequency at power command	16W (kHz)	30W (kHz)	34W (kHz)	56W (kHz)	68W (kHz)
T8-18	1.7	-	-	-	-
T8-32	0.004	0.816	-	-	-
T8-36	0.036	1.022	1.210	-	-
T8-58	0.002	0.288	0.444	0.476	-
T8-70	0.010	0.160	0.234	0.360	0.270

tioned range, there will be no damage for all T8 series lamps. If the lamp is turned off and turned back on while the filament temperature is still higher than the room temperature, a power control loop must be included to protect the filament

### 3. Electronic Ballast Controller Design

The operation of the electronic ballast system can be described as five stages: initialization, pre-heat, lamp detection, run, and stop. The flowchart of these operations is illustrated in Fig. 5. The block diagram of controller is shown in Fig. 6.

**3.1 Initialization state** During the initial phase, the controller sets the PWM frequency at 100 kHz and keeps it steady for 200 ms. This feature has been implemented to charge the blocking capacitor.

**3.2 Preheat state** The controller raises the frequency by one step every time the measured current is greater than the desired value, and lowers the frequency if the current is lower than the desired value. This state takes approximately 0.5 to 1 second depending on the current command value<sup>(19)</sup>.

**3.3 Ignition state** The controller decreases the frequency (increases the voltage) to ignite the lamp. Since the voltage across the lamp will significantly decrease after ignition because the current begins to flow through the lamp then, the voltage change is used as ignition indication. After detecting the ignition, the controller moves to the next phase.

**3.4 Stop state** If abnormal conditions occur, the software will automatically switch into the safety state that is designed to turn off the half bridge driver. Abnormal conditions may arise due to lamp bulb removal, lamp failure to ignite, over-current or over-voltage, or a rectifying effect (end of life).

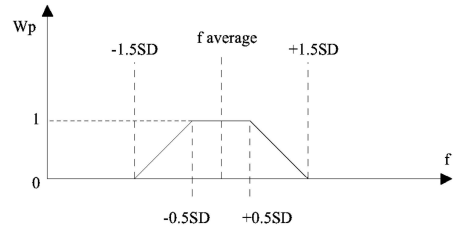


Fig. 9. Trapezoidal possibility weight ( $W_P$ ) VS running frequency

**3.5 Run state** During this phase, the controller measures the current required to deliver a given power to the lamp. The measured value is compared with a preset power command value, and consequently the software tries to correct any discrepancy. As mentioned above, the lamp power can be controlled by varying the operating frequency. The lamp power decreases when the supplied frequency increases, as shown in Fig. 2. The appropriate frequency must be generated to ensure that the connected lamp is not overdriven. The current regulation method is used to control the lamp power at its rating<sup>(20)</sup>. The average voltage across the series resistor on the low side of the driver MOSFET ( $V_{R_{sinv}}$ ) represents the inverter current ( $I_{inv}$ ).  $P_{inv}$ ,  $P_{lamp}$ , and  $I_{inv}$  are related as:

$$P_{inv} \propto P_{lamp} \propto I_{inv} \quad (12)$$

From (12), the lamp power can be controlled through  $V_{R_{sinv}}$ . Note that the required inverter power will be about 1-2 W less than the lamp rating for the same lumen output, due to the high frequency of operation.

**3.6 Lamp detection state** The lamp rating detection algorithm is composed of multi-step lamp power regulation and the trapezoidal possibility weight determination based on the lamp operating frequency. After ignition, the multi-step lamp power regulation is started with the lowest power command. For example, the 16W power command is used for the T8 series lamps. In the power control loop, the operating frequency is determined and collected in the controller. This frequency is used to classify the 18W (lowest) from the group. If the measured frequency is within the valid range, then no further decision is necessary and the controller proceeds to the running state. However, due to the variation between lamp manufacturers, bulb age, and temperature, the running frequency is not necessarily constant. We experimentally verified that the operating frequency varies during our lamp power regulation experiment.

Plenty of T8 lamps are operated at 16W, 30W, 34W, 56W and 68W to acquire the running frequencies. These frequencies are used in order to define the possibility weight function. Table 1 and 2 present the average and standard deviation of running frequency at 16 to 68 W of power regulation. A dash(-) symbol is a prohibited power command. By simplifying the Gaussian distribution, the trapezoidal possibility weight ( $W_P$ ) based on the operating frequency can be calculated from

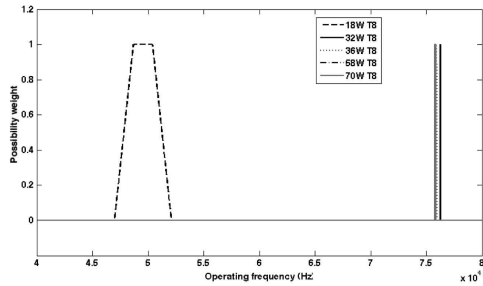


Fig. 10. Possibility weight ( $W_P$ ) VS operating frequency of T8 lamps at 16W power regulation

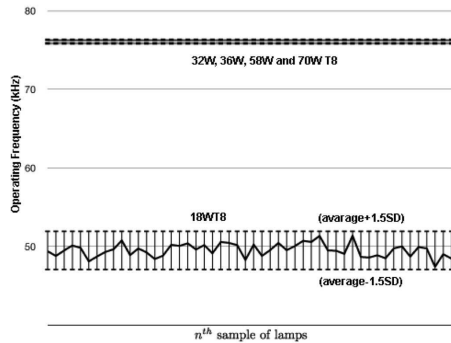


Fig. 11. Operating frequency at 16W power regulation of  $n^{th}$  lamp sample in the possibility weight region

$$W_P = \begin{cases} 1; \bar{f} - 0.5sd, f, \bar{f} + 0.5sd \\ \frac{1}{sd}f - \frac{\bar{f}-1.5sd}{sd}; \bar{f} - 1.5sd, f, \bar{f} - 0.5sd \\ \frac{-1}{sd}f + \frac{\bar{f}+1.5sd}{sd}; \bar{f} + 0.5sd, f, \bar{f} + 1.5sd \end{cases} \quad (13)$$

Where

$$\bar{f} = \frac{1}{n} \sum_{i=1}^n f_i, sd = \sqrt{\frac{1}{n} \sum_{i=1}^n (f_i - \bar{f})^2} \quad (14)$$

and  $n$ =number of samples,  $f_i$  = frequency of sample  $i$ .

The relation between the probability weight and the running frequency is illustrated in Fig. 9. For example, if the average operating frequency of a 36 W lamp running at 16 W is 75.88 kHz, and its standard deviation is 36 Hz, then  $W_{P(36W at 16W)}$  is

$$W_{P(36 at 16)} = \begin{cases} 1; 48.69kHz, f, 50.39kHz \\ 0.588f - 46.99; 46.99kHz, f, 48.69kHz \\ 0.588f + 50.39; 50.39kHz, f, 52.09kHz \end{cases} \quad (15)$$

where  $f$  = measure lamp operating frequency (kHz).

Fig. 10 and 11 shows the possibility weight and operating frequency of T8 series lamps at 16 W power regulation. The operating frequency of 18 W lamp is significantly far from others resulting in high accuracy of 18W lamp detection. However, the possibility weight of 58W lamp is overlapped by that of 32W lamp causing inaccurate detection in this state. When the 30 W power regulation is applied with the 32 W, 36 W, 58 W and 70 W T8 lamps, there is no overlapping in the possibility weight of T8 lamps as shown in Fig 12 and

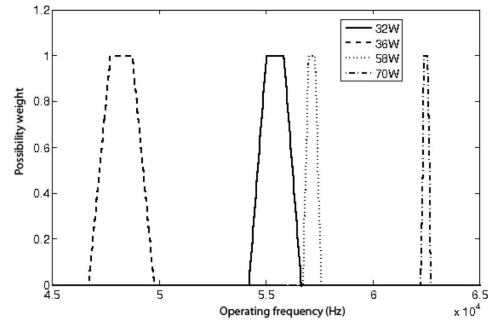


Fig. 12. Possibility weight ( $W_P$ ) VS operating frequency of T8 lamps at 30W power regulation

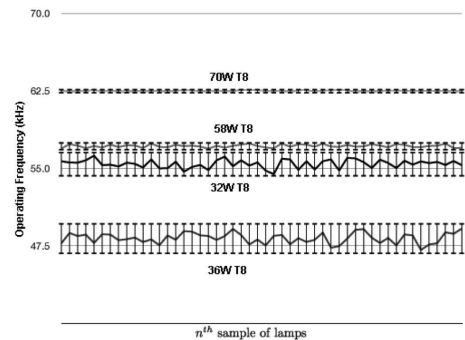


Fig. 13. Operating frequency at 30W power regulation of  $n^{th}$  lamp sample in the possibility weight region

13 where the 32 W lamp can be accurately detected.

From the reason above, both the multi-step lamp power regulation and possibility weight determination are applied together and the lamp rating detection algorithm can be described as follows:

- (1) Regulate at the lowest power command. Example: 16W for T8 series.
- (2) Calculate the probability weight for all lamp ratings. If the highest  $W_P$  is obtained at the lamp rating that equals the power command, the lamp rating equals the power regulated, then go to step 4.
- (3) If the delivered power is still below the lamp rating, step up to the next power command (30, 34, 56 and 68 W) and repeat step 1) and 2) again until the power command reaches the highest value of the series then go to step 4.
- (4) Summarize the total  $W_P$  of each lamp rating for each power regulation. The lamp rating is determined from the total highest  $W_P$ .

The flowchart of the detection algorithm is illustrated in Fig. 14.

**3.7 Discussions on Aging Effect** Regarding to the lamp aging, this might cause an increase in filament resistance, sputtering and filament damage respectively. The lamp discharge characteristics also change as well. After striking, the lamp with sputtering or filament damage will be shut off by the designed protection as previously stated. However, the aging effect from an increased filament resistance and lamp discharge char-

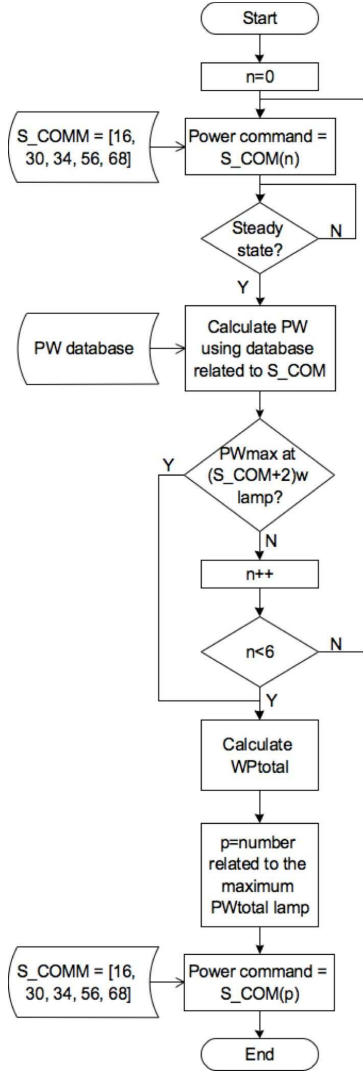


Fig. 14. Flowchart of the lamp rating detection algorithm

acteristics might cause the inaccurate detection. For example; the overlapped operating frequency of 32WT8 and 58WT8 might occur during the 30 W power regulation. In our designed ballast, the 18W, 32W and 36W T8 lamps, which are mostly used in our country, are selected. The operating frequencies of these lamps are quite far from each other causing the high accurate detection. Moreover, the cost of ballast can be reduced for not using the unnecessary high power components.

#### 4. Numerical calculation Results

The simplified resonant inverter is used in the simulation<sup>(24)</sup>. The controllable ac voltage source is connected through the resonant inductor and capacitor as a low-pass filter, with the fluorescent lamp as a resistive load ( $R_{lamp}$ ) as shown in Fig. 4. Using an operating frequency range from 25 kHz to 65 kHz, as described in<sup>(2)</sup>, and assuming that  $\eta_{inv}$  is 0.95 and  $V_{DC}$  is 400 V, the resonant inductance can be calculated by (6) which is given as 1.9 mH. With  $I_{ph}$  as 0.6 A and  $V_{ph}$  as 300 V, the substitution of the resonant inductance in (9) yields the resonant capacitance of 4.11nF. Because of com-

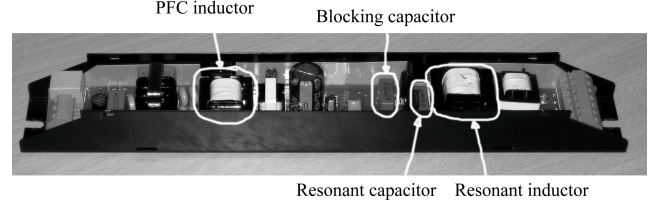


Fig. 15. A prototype of the multi-rating ballast

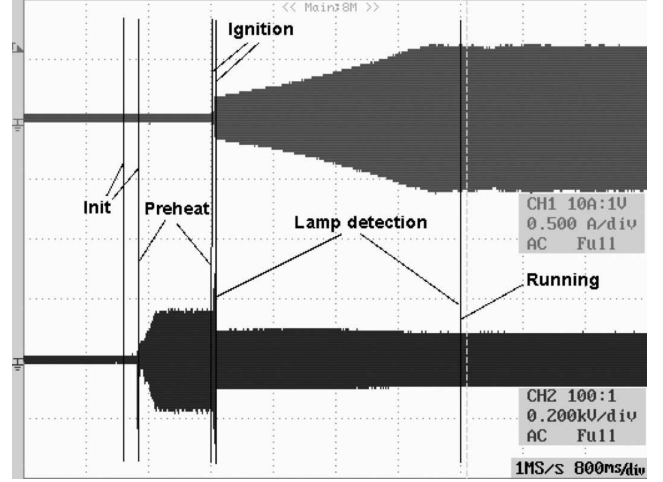


Fig. 16. The 36WT8 lamp current and voltage waveforms. Channel 1 is lamp current. Channel 2 is lamp voltage.

mercial availability, a capacitance of 4.7 nF is chosen. During the running stage, the lamp acts as a negative differential resistor<sup>(25)~(28)</sup>, which can be calculated as:

$$R_{lamp} = \frac{V_0 R_S}{V_0 - V_H} \quad (16)$$

where  $V_0$  is the voltage at present condition and  $R_S$  and  $V_H$  are defined as;

$$R_S = \frac{V_{Max} - V_{min}}{I_{Max} - I_{min}} \quad (17)$$

$$V_H = V_{min} - I_{min} R_S \quad (18)$$

where  $V_{max}$  is the lamp voltage at the highest power,  $V_{min}$  is the lamp voltage at the lowest power,  $I_{max}$  is the lamp current at the highest power, and  $I_{min}$  is the lamp current at the lowest power. Specifications for  $V_{max}$ ,  $V_{min}$ ,  $I_{max}$ , and  $I_{min}$  can be obtained from the lamp manufacturers. Because the higher-order harmonics only account for a small percentage of the input, the voltage and current waveforms appearing at the lamp are assumed to be sinusoidal. Considering only the fundamental component, lamp power ( $P_{Lamp}$ ) can be calculated as:

$$P_{lamp} = \left| \frac{-\frac{jV_{in}}{\omega C R_{lamp}}}{\left(j\omega L - \frac{j}{\omega C_{bl}}\right) \left(R_{lamp} - \frac{j}{\omega C}\right) - \frac{jR_{lamp}}{\omega C}} \right|^2 \quad (19)$$

Starting with an initial operating frequency, the lamp power is calculated. If  $P_{lamp}$  is less than the power

Table 3. Simulation result of  $W_P$  for the 32 W T8 lamp

Power command	16W	30W	34W	56W	68W	Sum
Lamp rating						
18W	0	-	-	-	-	0
32W	1	0.2	-	-	-	1.2
36W	0	0	-	-	-	0
58W	1	0	-	-	-	1
70W	0	0	-	-	-	0

Table 4. Experimental results of  $W_P$  for 58W lamp

Power command	16W	30W	34W	56W	68W	Sum
Lamp rating						
18W	0	-	-	-	-	0
32W	1	0	-	-	-	1
36W	0	0	0	-	-	0
58W	1	1	1	1	-	3
70W	0	0	0	0	-	0

command, the frequency is decreased and the lamp voltage, current, and resistance are recalculated at the new power level. The calculation is then iteratively repeated until the  $P_{lamp}$  is sufficiently close to the power command and the running frequency is obtained. The simulation result for the probability weight calculation for the 32W T8 lamp is shown in Table 3. Starting at the 16W power command, the running frequency is 76.26 kHz and  $W_P$  at 16 W is calculated. The highest  $W_P$  is not at  $W_{P_{18W at 16W}}$ , thus the 30W power command is regulated and  $W_P$  at 30 W is recalculated. The algorithm stops at 30W power command due to the maximum on  $W_{P_{32W at 30W}}$ . The summation of  $W_{P_{32W}}$  is 1.2, which is the maximum, and the lamp is detected as a 32W rated lamp.

## 5. Experiment Results

A hardware prototype of the electronic ballast, shown in Fig. 15, was built. The values for the resonant inductance and capacitance match those used in the simulation. The PFC boost inductance and the DC bus capacitance are 0.94 mH and 22  $\mu$ F, respectively. A 100 nF blocking capacitor is used. Fig. 16 shows the ballast operation with the 36W lamps.

In the preheat state, the controller maintains the lamp current and voltage at 600 mA and 300 V, respectively. After striking, the lamp power is regulated according to the lamp rating detection algorithm. All tested lamps have been successfully detected at their ratings. The startup process, including lamp detection, takes approximately 3 to 40 seconds. The sample of detection results for a 58W T8 lamp is shown in Table 4.

The voltage detection is the commonly used method in detecting ballasts rating<sup>(10) (11)</sup>. With different power ratings, the lamp resistances may be different and the lamp peak voltages after strikes may be used to classify the power ratings. However, this may not be the case for T8 series because the lamp peak voltages of differ-

Table 5. Detecting results of T8 lamp at 16W, 30W, 34W, 56W and 68W power regulation state

Lamp rating	18W	32W	36W	58W	70W
16W power regulation					
% Detection rates	100	90	90	20	36
% Type I error	0	10	10	80	64
% Type II error	0	2	0	32	0
30W power regulation					
% Detection rates	-	100	100	100	98
% Type I error	-	0	0	0	2
% Type II error	-	0	0	0	0
34W power regulation					
% Detection rates	-	-	100	100	100
% Type I error	-	-	0	0	0
% Type II error	-	-	0	0	0
56W power regulation					
% Detection rates	-	-	-	100	100
% Type I error	-	-	-	0	0
% Type II error	-	-	-	0	0
68W power regulation					
% Detection rates	-	-	-	-	100
% Type I error	-	-	-	-	0
% Type II error	-	-	-	-	0

ent ratings can and have been found to be in the same range. In Fig. 17, the lamp voltages are obtained from 50 samples of each of the T8 series lamp rating with the total number of 250 lamps. The voltages after strikes of the 32W and 58W lamps are located in the ranges of 162 V to 177 V and 166 V to 177 V, respectively. The detection result is very likely to be incorrect for both lamp ratings. This method yields the result of detection rate as 86%.

To evaluate this proposed method, hundreds of arbitrarily chosen fluorescent lamps with varied age are tested with proposed ballast. The operating frequencies of tested lamps at 16W and 30W power regulation are shown in Fig. 11 and 13, respectively. At 30W power regulation, the operating frequencies of all lamps are in the areas of their possibility weight. Thus, the proposed method can distinguish between 32W and 58W lamps. Note that some lamps with low possibility weight might have the chance of type I error (the false positive - the error of rejecting lamp when it is actually at rating) as well as the type II error (the false negative - the error of failing to reject a lamp when it is in fact not at rating). Even though the 16W power regulation state returns 100%-accuracy 18W lamps detection, this state returns detection errors for the other ratings. Table 5 shows the lamp detection rate, type I error rate and type II error rate of T8 lamps at various power regulations.

The proposed frequency detection, on the other hand, uses the frequency command for lamp power regulation to detect the lamp power. This frequency command is the same frequency command that is used to regulate the lamp power in order to avoid overdriven condition. Together with the proposed possibility weight functions,

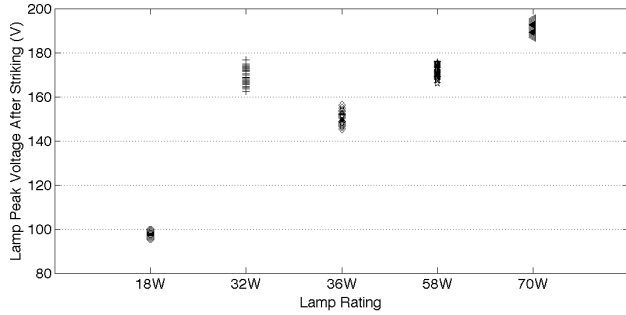


Fig. 17. Relationship between lamp voltages and ratings after strikes

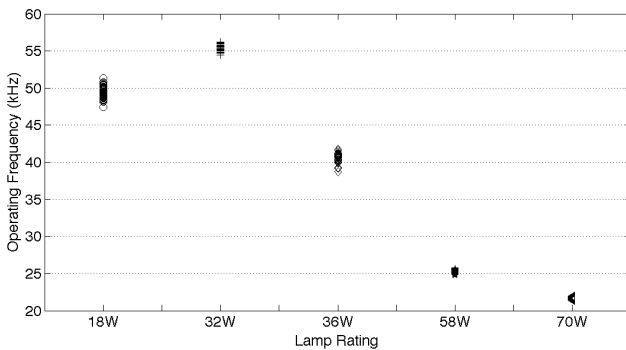


Fig. 18. Relationship between lamp frequencies and ratings from power regulation

the operating frequencies of each lamp rating are obtained from the multi-stage power regulation starting from the lowest rating available as shown in Fig. 18. With the same set of 250 lamps used in obtaining the results in Fig. 17, the operating frequency range of each rating is located apart from each other. Clearly, the frequency detection method does not suffer from overlapping range of the detection parameter. The detection results of the proposed method are evidently more accurate. It is worth noting that if a delay of 10s is added before obtaining the operating frequency, 100% detection accuracy may be achieved since the lamp resistance is allowed to reach its stable state.

The important advantage of implementing the proposed frequency detection method is that the frequency command to be used in the detection process is sent out from the controller. Unlike the voltage detection, the detecting parameter does not need to go through sensing circuitry and the analog-to-digital conversion process. Therefore, it is not subjected to external noise which can worsen the detection results.

From table 5, the lamp detection rate, type I error rate and type II error rate are calculated as:

$$D.R. = \frac{N_{Correct}}{N_{Lamp}} \times 100 \quad (20)$$

where D.R. is detection rate,  $N_{Correct}$  is number of the accurately detected lamps and  $N_{Lamp}$  is number of tested lamp.

$$TypeI = \frac{N_{Reject}}{N_{Lamp}} \times 100 \quad (21)$$

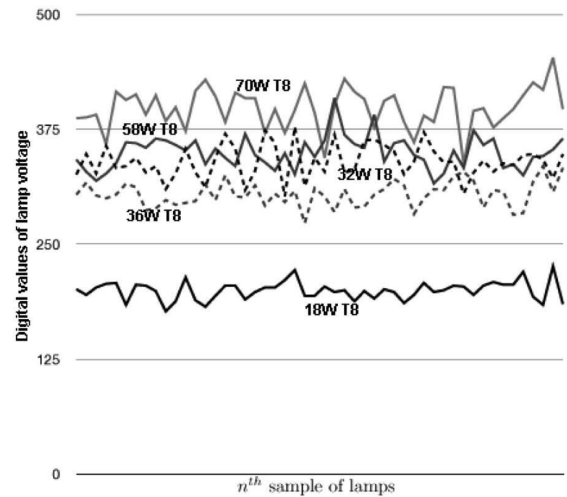


Fig. 19. Peak voltage of  $n^{th}$  sample of lamps after ignition using the micro-controller analog to digital converter

Table 6. Voltage detecting method (V.D.) VS Proposed frequency detecting method results

Lamp rating	18W	32W	36W	58W	70W
V.D. Method					
% Detection rates	100	60	100	70	100
% Type I error	0	40	0	30	0
% Type II error	0	30	0	40	0
Proposed method					
Lamp rating	18W	32W	36W	58W	70W
% Detection rates	100	100	100	100	100
% Type I error	0	0	0	0	0
% Type II error	0	0	0	0	0

where  $N_{Reject}$  is number of lamps that are rejected when it is actually at its rating.

$$TypeII = \frac{N_{WrongAccept}}{N_{Lamp}} \times 100 \quad (22)$$

where  $N_{WrongAccept}$  is number of lamps that are accepted when it is not at its rating.

Because of the overlapped possibility weight of the 32 W and 58 W lamp, the high type I and type II error of 58W lamps are occurred during 16W power regulation. Even the low accuracy occurs in 16W power regulation state, the next power regulation state results in the high detection accuracy implying the right rating will be detected at the final decision. Therefore, this algorithm results in a 100% detection rate of all tested lamps. For the testing with very old lamps, the inaccurate detection is occurred but the protection algorithm stops the ballast operation due to the rectifying effect.

Comparing the proposed detection with the voltage detection method, the experiment for measuring lamp voltages after ignition are carried out as shown in Fig. 17. Using this method, the 70W and 18W lamps are easily detected but the detection between 32W and 58W lamps is not possible. The main reason is that the lamp

voltage after ignition varies with the lamp temperature, age, and manufacturer. Moreover, the use of A/D converter in micro-controller will cause the noise amplification as shown in Fig. 19. The noisy switching environment will worsen the detection accuracy. With the proposed method, the frequency is generating by the micro-controller itself which is not interfered by noise. And the multi-step power regulation constrains the lamp operating condition during the detection as well. The Detection results of the proposed method and the voltage detecting method are shown in Table 6.

## 6. Conclusion

A multi-rating electronic ballast for fluorescent lamps based on operating frequency determination has been presented. The detection algorithm is based on the probability weight distribution of the lamp operating frequency, and multi-step lamp power regulation. The proposed algorithm has shown great accuracy in detecting the targeted lamp power rating compared with the commonly used voltage detection method. In some cases, aging lamps may result in misclassification of the lamps therefore, a protection circuit must be implemented with the ballast. With the proposed detection algorithm, the multi-rating ballast will help eliminate concerns about matching the ballast circuit with the designated lamp power rating.

## References

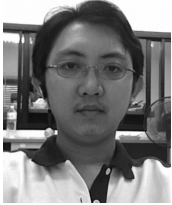
- (1) L. Davies, H. Ruff, and W. Scott, "Fluorescent lamps," *Electrical Engineers - Part II: Power Engineering, Journal of the Institution of*, vol. 89, pp. 447–465, October 1942.
- (2) I. John, E. Kaufman, and J. F. Christensen, *IES Lighting Handbook*. Illuminating Engineering Society, 1984.
- (3) M. Kazimierczuk and W. Szaraniec, "Electronic ballast for fluorescent lamps," *IEEE Transactions on Power Electronics*, vol. 8, pp. 386–395, Oct 1993.
- (4) M. Matsuo, T. Suetsugu, S. Mori, and I. Sasase, "Class de current-source parallel resonant inverter," *Industrial Electronics, IEEE Transactions on*, vol. 46, pp. 242–248, Apr 1999.
- (5) J. Cosby, M.C. and R. Nelms, "A resonant inverter for electronic ballast applications," *Industrial Electronics, IEEE Transactions on*, vol. 41, pp. 418–425, Aug 1994.
- (6) C. Liu, F. Teng, C. Hu, and Z. Zhang, "Lcl resonant converter for multiple lamp operation ballast," *Applied Power Electronics Conference and Exposition, 2003. APEC '03. Eighteenth Annual IEEE*, vol. 2, pp. 1209–1213 vol.2, Feb. 2003.
- (7) J. Alonso, J. Cardesin, Calleja, Rico-Secades, and J. Garcia, "A fluorescent lamp electronic ballast for railway applications based on low-cost microcontroller," *IEEE Transactions on Industry Applications*, vol. 41, pp. 1391–1400, Sept.-Oct. 2005.
- (8) R.-L. Lin and Y.-T. Chen, "Electronic ballast for fluorescent lamps with phase-locked loop control scheme," *IEEE Transactions on Power Electronics*, vol. 21, pp. 254–262, Jan. 2006.
- (9) Y. Ji, R. Davis, C. O'Rourke, and E. Chui, "Compatibility testing of fluorescent lamp and ballast systems," *Industry Applications, IEEE Transactions on*, vol. 35, pp. 1271–1276, Nov/Dec 1999.
- (10) L. Lee, S. Hui, and H. Chung, "An automatic lamp detection technique for electronic ballasts," *Twentieth Annual IEEE Applied Power Electronics Conference and Exposition, 2005. APEC 2005*, vol. 1, pp. 575–581 Vol. 1, March 2005.
- (11) L.-M. Lee and S. Hui, "Automatic lamp detection and operation for warm-start tubular fluorescent lamps," *IEEE Transactions on Power Electronics*, vol. 24, pp. 2933–2941, dec. 2009.
- (12) S.-M. Chen, Y.-K. Ko, Y.-C. Chang, and J.-S. Pan, "Weighted fuzzy interpolative reasoning based on weighted increment transformation and weighted ratio transformation techniques," *Fuzzy Systems, IEEE Transactions on*, vol. 17, pp. 1412–1427, Dec. 2009.
- (13) T.-F. Wu, Y.-C. Liu, and Y.-J. Wu, "High-efficiency low-stress electronic dimming ballast for multiple fluorescent lamps," *Power Electronics, IEEE Transactions on*, vol. 14, pp. 160–167, Jan 1999.
- (14) T.-F. Wu and T.-H. Yu, "An electronic dimming ballast with bifrequency and fuzzy logic control," *Industry Applications, IEEE Transactions on*, vol. 36, pp. 1308–1317, Sep/Oct 2000.
- (15) I. R. Corporation, "I.R. ballast designer version 4.1.7." PC Software, 2006.
- (16) T. Ribarich and J. Ribarich, "A new procedure for high-frequency electronic ballast design," *IEEE Transactions on Industry Applications*, vol. 37, pp. 262–267, Jan/Feb 2001.
- (17) S. S. M. Chan, H. S.-H. Chung, and Y.-S. Lee, "Design and implementation of dimmable electronic ballast based on integrated inductor," *Power Electronics, IEEE Transactions on*, vol. 22, pp. 291–300, Jan. 2007.
- (18) H. Sartori, H. Hey, and J. Pinheiro, "An optimum design of pfc boost converters," in *EPE '09. 13th European Conference on Power Electronics and Applications, 2009.*, pp. 1–10, Sept. 2009.
- (19) F. Wakabayashi, M. de Brito, C. Ferreira, and C. Canesin, "Setting the preheating and steady-state operation of electronic ballasts, considering electrodes of hot-cathode fluorescent lamps," *Power Electronics, IEEE Transactions on*, vol. 22, pp. 899–911, May 2007.
- (20) D. Klien, "A sensing and regulation concept for high end dimming ballasts," in *38th IAS Annual Meeting. Conference Record of the Industry Applications Conference, 2003.*, vol. 2, pp. 785–790 vol.2, Oct. 2003.
- (21) Y. Ji, R. Davis, C. O'Rourke, and E. Chui, "Compatibility testing of fluorescent lamp and ballast systems," *IEEE Transactions on Industry Applications*, vol. 35, pp. 1271–1276, Nov/Dec 1999.
- (22) *American National Standard for Ballasts for Fluorescent Lamps: Specifications*, ANSI C82.1-1985, 1985.
- (23) P. Tam, S. Lee, S. Hui, and H.-H. Chung, "Practical evaluation of dimming control methods for electronic ballasts," *Power Electronics, IEEE Transactions on*, vol. 21, pp. 1769–1775, Nov. 2006.
- (24) Z. Li, P. Mok, W.-H. Ki, and J. Sin, "A simple method to design resonant circuits of electronic ballast for fluorescent lamps," *ISCAS '97., Proceedings of 1997 IEEE International Symposium on Circuits and Systems.*, vol. 3, pp. 1744–1747 vol.3, Jun 1997.
- (25) A. Ng, W.-H. Ki, P. Mok, and J. Sin, "Lamp modeling for design of dimmable electronic ballasts," *2000 IEEE 31st Annual Power Electronics Specialists Conference, 2000. PESC 00.*, vol. 3, pp. 1358–1362 vol.3, 2000.
- (26) S. Glozman and S. Ben-Yaakov, "Dynamic interaction analysis of hf ballasts and fluorescent lamps based on envelope simulation," *Industry Applications, IEEE Transactions on*, vol. 37, pp. 1531–1536, Sep/Oct 2001.
- (27) T.-F. Wu, J.-C. Hung, and T.-H. Yu, "A ps Spice model for fluorescent lamps operated at high frequencies," *21st International Conference on Industrial Electronics, Control, and Instrumentation, 1995., Proceedings of the 1995 IEEE IECON*, vol. 1, pp. 359–364 vol.1, Nov 1995.
- (28) M. Sun and B. Hesterman, "Pspice high-frequency dynamic fluorescent lamp model," *Power Electronics, IEEE Transactions on*, vol. 13, pp. 261–272, Mar 1998.

---

## Acknowledgment

This work was supported by the Higher Education Research Promotion and National Research University Project of Thailand , Office of the Higher Education Commission.

**Piyasawat Navaratana Na Ayudhya** (Non-member) was



born in Bangkok, Thailand, on April 8, 1976. He received the B.E. and M.E. degrees in electronic and telecommunication engineering from King Mongkut's University of Technology Thonburi (KMUTT), Bangkok, Thailand, in 1997 and 2000, respectively. Since 2000, he has been a Lecturer in the Electrical Engineering Department, King Mongkut's University of Technology Thonburi, teaching digital techniques and micorcontroller system. Since 2004, he has also been a consultant of DYNO electric Co.,Ltd., Nakornpatom, Thailand. His research interests include electronic ballast, battery charger, switching power supplies, digital signal processing and machine intelligence.

**Sumate Naetiladdanon** (Non-member) received the B.Eng. degree from Chulalongkorn University, Bangkok,



Thailand, in 1995, the M.Sc. degree from Rensselaer Polytechnic Institute, NY, USA., in 1999, and the Ph.D. degree from Osaka University, Japan in 2006. He is currently a Lecturer in the Department of Electrical Engineering of King Monkuts University of Technology Thonburi (KMUTT). His research interests are in the areas of power electronics for power quality improvement and renewable energy.

**Anawach Sangswang** (Non-member) received the B.Eng.



degree from King Mongkuts University of Technology Thonburi (KMUTT), Bangkok, Thailand, in 1995, and the M.S. and Ph.D. degrees from Drexel University, Philadelphia, PA, in 1999 and 2003, respectively. He is currently a Lecturer in the Department of Electrical Engineering, KMUTT. His research interests include stochastic modeling and digital control of power electronic converters. His recent work has been in the application of PV gridconnected systems and power distribution systems.